

# Doxorubicin-liposome combined with clodronate-liposome inhibits hepatocellular carcinoma through the depletion of macrophages and tumor cells

Li Zhang

lizhangpaper@163.com

Changhai Hospital, Naval Medical University

Hengyan Zhang

Changhai Hospital, Naval Medical University

Dandan Sheng

PLA Strategic Support Force Medical Center

Xiaojuan Hou

Third Affiliated Hospital of Second Military Medical University

Gangqi Sun

Changhai Hospital, Naval Medical University

Luyao Zhang

Changhai Hospital, Naval Medical University

Xue Yang

Third Affiliated Hospital of Second Military Medical University

Xinxia Wang

Shanghai International Medical Center, Shanghai International Medical Center

Lixin Wei

Third Affiliated Hospital of Second Military Medical University

Ying Lu

Naval Medical University

Zhipeng Han

Third Affiliated Hospital of Second Military Medical University

---

## Research Article

**Keywords:** Hepatocellular carcinoma, Chemotherapy, Doxorubicin, Liposomes, Doxorubicin-liposome, Clodronate-liposome, Macrophages, Hepatic progenitor cells

**Posted Date:** April 27th, 2022

**DOI:** <https://doi.org/10.21203/rs.3.rs-1582891/v1>

**License:**  This work is licensed under a Creative Commons Attribution 4.0 International License.

[Read Full License](#)

**Additional Declarations:** No competing interests reported.

---

**Version of Record:** A version of this preprint was published at International Journal of Pharmaceutics on December 1st, 2022. See the published version at <https://doi.org/10.1016/j.ijpharm.2022.122346>.

# Abstract

**Background:** Macrophages in the liver have capacities of capturing and phagocytosing nanocarriers and play an important role in inflammatory microenvironment and hepatocellular carcinoma (HCC) initiation and progression. Depletion of macrophages might be a feasible strategy for drug delivery and tumor microenvironment modulation during HCC.

**Methods:** To verify this hypothesis, liposomes targeting macrophages containing DOX and clodronate were prepared using ammonium sulfate gradient and thin film hydration method. Then liposomes were given to rats at different stages of diethylnitrosamine (DEN) induced primary HCC model to understand the preventive and therapeutic effects of the liposomes.

**Results:** Doxorubicin-liposome (Doxil) and clodronate-liposome (CL-LIP) about 180-200 nm were successfully prepared and characterized, with a polydispersity index of <0.3 and free doxorubicin (DOX) encapsulation efficacy of >97%. We found that Doxil combined with CL-LIP could effectively target and eliminate macrophages in the liver, releasing DOX into plasma and inhibiting HCC *in vivo*.

**Conclusions:** DOX and clodronate-loaded liposomes targeting macrophages can effectively reduce macrophages phagocytosis, concentrate DOX in the plasma and accumulate DOX in the liver and spleen for a longer time, improving tumor microenvironment and restraining activation of hepatic progenitor cells (HPCs), thus enhance the inhibition and therapeutic effects against HCC in rats. Results of this study were expected to provide a new prospect for the chemotherapy of HCC.

## Background

Hepatocellular carcinoma (HCC) has become a common cause of death in cancer patients and a great health burden worldwide<sup>1,2</sup>. Traditional anti-cancer drugs, such as Doxorubicin (DOX), 5-Fluorouracil, Pirarubicin and Cisplatin, have been routinely used for clinical HCC treatments. However, multi-organ toxicity and drug resistance greatly limited their clinical application. With the development of nanotechnology, nanoparticles loaded with chemotherapeutic drugs have been designed to reduce toxicity and increase therapeutic efficacy. Liposomes, one of the most widely used nanoparticle forms, have high biocompatibility, good pharmacokinetic properties, easy surface modification and long cycle time after surface or size modification(1, 2). However, liposomes are quickly recognized and eliminated by mononuclear phagocytic system (MPS) after entering the body. MPS can greatly reduce the drug delivery efficiency to tumor tissues and accumulate liposomes in MPS organs, resulting in unsatisfactory therapeutic effect<sup>5-7</sup>.

Liver is one of the main MPS organs and contains abundant macrophages(3). HCC is known to be an inflammatory-related disease. Macrophages, as the main component of inflammatory microenvironment and immune process(4, 5), play a critical role in maintaining normal liver physiology homeostasis and removing harmful substances, pathogens and damaged or abnormal tissues, including liposomes(6). Under pathological state, macrophages are involved in the initiation, progression and metastasis of

HCC(7–10). Macrophages could promote malignant transformation of HCC by supporting angiogenesis(11) and creating immunosuppressive environment. Tumor-associated macrophage (TAM) accumulation was found in the liver of HCC patients and is associated with poor progression and low survival of HCC. Clinical researches showed that high density infiltration of macrophages in tumor was closely related to the poor prognosis of HCC patients(12, 13). Therefore, we wondered whether the phagocytosis of liposomes by macrophages in the liver can be utilized to treat HCC and whether depletion of macrophages could promote the delivery of drug-loaded liposomes to targeted tissue or cells.

In this research, liposomes targeting and exhausting macrophages containing DOX and clodronate were prepared according to the features of macrophages in the liver. DOX is a widely used broad-spectrum antitumor drug to treat solid tumors by inhibiting DNA and protein synthesis(14, 15). Clodronate is a bisphosphonates drug and has become a common strategy for exhaustion of macrophages *in vivo*, mainly by its liposome form. Clodronate liposomes can effectively deplete macrophages in different organs or tissues, including the liver(16). In this study liposomes were prepared and characterized, and then administered at different stages of primary HCC model in rats, so as to understand their effects on hepatocarcinogenesis, tumor development and microenvironment. To the best of our knowledge, this is the first attempt to deplete macrophages for HCC treatment by local injection of mixed liposomes into the liver through spleen, and the results of the study are expected to provide a new strategy for the prevention, treatment and anti-postoperative recurrence of HCC.

## Methods

### Reagents

Doxorubicin, cholesterol and diethylnitrosamine (DEN) were purchased from SIGMA-Aldrich (St. Louis, MO, USA). Egg yolk lecithin E80 was purchased from Lipoid GmbH (Ludwigshafen, Germany). For cells culture, Ham's F-12K, RPMI 1640 and DMEM media were all acquired from Gibco/Life Technologies (Grand Island, NY, USA). Anti-CD68, anti-CD163, anti-iNOS, and anti-Alpha-fetoprotein (AFP) antibodies were obtained from Abcam (Cambridge, MA, USA). Anti-OV6 antibody was bought from R&D (Minneapolis, MN, USA). Becton, Dickinson and Company (Franklin Lakes, NJ, USA) provided the FITC Annexin V Apoptosis Detection Kit. Servicebio (Wuhan, China) provided the cell counting Kit-8 (CCK8) and ELISA assay kits were all from Nanjing Jiancheng Bioengineering Institute (Nanjing, China). All other reagents such as alcohol, chloroform used in this study were of analytical grade from commercial sources.

### Animals and Cells

Male Sprague-Dawley (SD) rats weighing 180-200g were purchased from Shanghai Animal Experimental Center of Chinese Academy of Sciences (Shanghai Slack Experimental Animal Co., LTD., China), and maintained under pathogen-free conditions with a 12 h light and 12 h dark cycle in the Second Military Medical University Animal Care Committee. After one week of adaptive feeding, rats were given 0.1% DEN

in their drinking water to induce hepatocarcinoma, along with a standard diet. All animal protocols used were approved by the Institutional Animal Care and Use Committee of the Institute of Health Sciences.

Rat alveolar macrophages (NR8383) and rat hepatocytes (RH35) cell lines were both purchased from Cell Bank of Chinese Academy of Sciences (Shanghai, China).

### Preparation and Characterization

Doxorubicin-liposomes (Doxil) with different sizes were prepared by reverse phase evaporation vesicle (REV) and ammonium sulphate gradient method(17-19). High Performance Liquid Chromatography (HPLC) was performed on a Dionex UltiMate 3000 system (Waltham, MA, USA) to determine the concentration of doxorubicin. Agilent ZORBAX-SB-C18 column (5  $\mu$ m, 4.6  $\times$  150 mm) were used at 35  $^{\circ}$ C. Gradient elution system was composed of (A) 76% 0.1% aqueous triethylamine (pH=3.0) and (B) 24% acetonitrile as mobile phase. The encapsulation efficiency (EE%) and drug loading (DL%) were calculated according to the equations below:

$$EE(\%) = \frac{W_{loaded\ drug}}{W_{total\ drug}} \times 100\%$$

$$DL(\%) = \frac{W_{loaded\ drug}}{W_{liposomes}} \times 100\%$$

Clodronate-liposome (CL-LIP) was successfully prepared using thin film hydration method(20) and its concentration was detected by ultraviolet spectroscopy at 240 nm described previously(21). Liposomes' particle sizes, Zeta potentials, polydispersity index (PDI) and stability in a week were measured by a dynamic light scatterer (Malvern Zetasizer, Malvern, UK). The cumulative release rates of DOX at 10 min, 20 min, 30 min, 1 h, 4 h, 8 h, 12 h, 24 h, 48 h, 72 h from different sizes of Doxil *in vitro* (PBS, pH=7.4) were detected by recording the fluorescence values of Doxil before and after demulsification ( $F_{initial}$  &  $F_{Triton\ X-100}$ ). Cumulative release rate of DOX was calculated using the equation below:

$$DOX\ Release\ Rate(\%) = \frac{(F - F_{initial})}{(F_{Triton\ X-100} - F_{initial})} \times 100\%$$

The images of Doxil and CL-LIP were recorded by a Tecnai G<sup>2</sup> F20 S-TWIN High-Resolution Transmission Electron Microscope (HRTEM, FEI, Hillsboro, OR, USA).

### Cell Culture and Treatment

Rat macrophages line NR8383 was cultured in Ham's F-12K medium (10% FBS) in incubators at 37 °C and 5% CO<sub>2</sub>. Rats whose peritoneal macrophages to be isolated were first activated by intraperitoneal injection of broth 5-7 days in advance. Then rats were injected intraperitoneally with RPMI 1640 (1% penicillin–streptomycin) after sacrifice and sterilization. Rat abdomen was kneaded gently and liquid inside was extracted for 1000rpm, 5 minutes centrifugation. Cells were then rinsed by medium and counted before resuspended and seeded to the culture plate. Non-adherent cells were removed after 2 h and adherent cells were maintained. The isolated peritoneal macrophages were cultured in RPMI 1640 medium (10% FBS) at 37 °C and 5% CO<sub>2</sub> and were identified by immunofluorescence staining.

NR8383 cells were treated with CL-LIP at concentrations of 5,10, 20 or 50 µg/mL for 24 h. Rat peritoneal macrophages were treated with CL-LIP at concentrations of 5, 10, 20,50, 100, 200 or 300 µg/mL for 24 h. Cell viability was estimated using CCK-8 assay according to the manufacturer's instructions.

Rat hepatocytes, RH35 cells were cultured in DMEM medium (10% FBS) in incubators at 37 °C and 5% CO<sub>2</sub>. Then RH35 cells were treated with PBS, CL-LIP (10 µg/mL), Doxil (1 µg/mL), Doxil+CL-LIP for 24h, and cell viability was estimated using CCK-8 assays.

### **Flow Cytometry Assay**

To estimate the depletion effects of CL-LIP on macrophages *in vitro*, the apoptosis of rat peritoneal macrophages following treatment with CL-LIP of different concentrations (5, 10, 20, 50, 100, 200 or 300 µg/mL) for 24 h were detected using FITC Annexin V-PI Apoptosis detection kit (BD Pharmingen, USA) and measured by flow cytometry.

### **Cell uptake and Immunofluorescence Assay**

To investigate the cell uptake efficiencies of Doxil of different sizes, rat peritoneal macrophages cells were seeded into culture plate with the addition of 10 µl Doxil (2 mg/mL) of 100, 200 nm and incubated for 0.5 h. Thereafter, the supernate was discarded, cells were washed by saline and the nuclei were counterstained with 4,6-diamidino-2-phenylindole (DAPI, Beyotime technology, Jiangsu, China) for 10 min before observing the cells by laser scanning confocal microscopy (LSCM).

To assess cell uptake ability of different sizes of Doxil *in vivo*, we chose HCC rats induced with DEN for 4 weeks, when the majority of macrophages in livers are activated. Rats were injected with 100, 200 nm Doxil (2 mg/Kg) through the spleen and livers were harvested after 1.5 h with attention to keep in the dark and stored at -80 °C to make frozen section. After incubated with indicated primary antibody, CD68(1:200, Abcam), sections were incubated with Alexa Fluor 488-labeled secondary antibodies (Invitrogen). Nuclei were counterstained with DAPI and then observed under a LSCM for immunofluorescence (IF) analysis.

### ***in Vivo* Toxicity Assay**

The *in vivo* toxicity of Doxil and CL-LIP was evaluated using DEN-induced HCC rats at 12 weeks. In brief, we injected different doses of Doxil (1, 2, 4 mg/kg) and CL-LIP (1, 5, 15, 35, 45 mg/kg) into 12-week-HCC-

induced SD rats once a week via the spleen for 4 weeks. Each dosage group had 3 animals. At the same time, saline was administered into the rats' spleen in the same manner to establish the DEN group. The survival rats were monitored daily.

To examine the *in vivo* toxicity of Doxil and CL-LIP, 1 week after injection, we harvested the livers and blood from rats in all groups and immersed livers in 4 % paraformaldehyde. Then the livers were paraffin-embedded, sectioned, and stained with hematoxylin and eosin (H&E). A confocal microscope (Leica TCS SP2, Germany) was used to observe the histological sections. Both the identity and analytical results of the pathology slides were unknown to the pathologist. Rat serum was extracted by centrifugation at 3000 rpm for 10 min and stored at -80 °C for biochemical analysis. Serum ALT, AST and ALB levels were determined using ELISA assay kits according to the manufacturer's instructions.

### **Treatment of Animals**

HCC rat models were established by DEN given in the drinking water. To observe the prevention and treatment influence of Doxil combined with CL-LIP in HCC, rats were divided into four groups: a. DEN; b. DEN+CL-LIP; c. DEN+Doxil; and d. DEN+CL-LIP+Doxil, with 5 animals in each group. The rats in four groups were administered with saline, CL-LIP (15 mg/kg), Doxil (2mg/kg) or Doxil (2mg/kg)+CL-LIP (15 mg/kg) once a week before hepatocarcinogenesis (8<sup>th</sup> to 11<sup>th</sup> week HCC-induced by DEN, **Fig. 2A**) and during liver cancer progression (14<sup>th</sup> to 17<sup>th</sup> week HCC-induced by DEN, **Fig. 5A**). The numbers of survival rats were recorded after administration starting from 14<sup>th</sup> to 17<sup>th</sup> week and Kaplan-Meier plot of DEN-induced rats was plotted during HCC progression (about 28 days).

Two batches of rats were sacrificed at 12<sup>th</sup> and 19<sup>th</sup> week since drinking DEN water severally. To further assess the effects of mixed liposomes on hepatocarcinoma, blood samples were drawn from IVC and were placed in coagulation-promoting tubes, and serum was separated by centrifugation at 3000 rpm for 10 min. All of the serum samples were stored at -80 °C until analysis. After rats were sacrificed, livers were excised and rinsed thoroughly with saline to remove residual blood and other contents. Liver tumors were measured with vernier caliper and counted. Then two hepatic lobes were cut and stored in 4 % paraformaldehyde, while the rest was divided into pieces and dried to be kept at -80 °C for subsequent experiments.

### **Hematoxylin-eosin (H&E) Staining, Immunohistochemistry, Terminal Deoxynucleotidyl Transferase-mediated dUTP-biotin Nick End Labeling (TUNEL) Assay and Image Analysis**

For histological examination, 3-5µm sections were cut from livers embedded in paraffin and stained with H&E according to the manufacturer's protocol. For immunohistochemical staining, the primary immunohistochemistry antibodies including AFP (1:100, Abcam), CD68 (1:200, Abcam), and OV6(1:50, R&D), CK19(1:200, Abcam) were used. Nuclei were counterstained with hematoxylin to demonstrate blue. The sections were subsequently scanned with a confocal microscope (Leica TCS SP2, Germany).

We used TUNEL staining (Calbiochem, La Jolla, CA, USA) to estimate the apoptosis level of liver tumor cells according to the manufacturer's instructions. Then the sections were stained with DAPI as counterstaining and observed under a LSCM.

### **Bio-distribution of Free Doxorubicin, Doxil and CL-LIP and Pharmacokinetic Analysis**

To observe the bio-distribution of Free doxorubicin and liposomes and the effects of CL-LIP on Doxil release *in vivo*, we established DEN induced primary liver cancer models in rats and prepared Doxil and CL-LIP. After feeding rats with DEN in drinking water for 8 weeks, Free doxorubicin, Doxil and mixed liposomes (Doxil+CL-LIP) were injected into the spleen. The dose of doxorubicin was 2 mg/kg in all the groups and clodronate was 15 mg/kg in Doxil+CL-LIP group. High Performance Liquid Chromatography-Mass Spectrometry (HPLC-MS) instrument, Waters ACQUITY H-Class UPLC/Xevo TQS (Framingham, MA, USA) was applied to detect the concentrations of doxorubicin in major organs like the heart, liver, spleen, lung, kidney and plasma at 0.5, 1, 2, 4, 8, 12, 24, 48 h after administration respectively. Rats were anesthetized before blood was drawn from IVC and organs were harvested at specific time points. Plasma extracted and organs were stored at -80 °C before HPLC-MS detection. The organs samples were pre-treated by grinding. Bio-distribution or accumulation of doxorubicin of rats was tracked at each time point using the HPLC-MS and concentration of doxorubicin in tissues and plasma were measured for further analysis (at least three samples of each rat were measured). HPLC-MS equipment and conditions are listed in detail in **supplementary materials**.

Pharmacokinetic analysis was done by DAS 3.3.0 software.

### **Statistical Analysis**

Statistical analysis was performed using Graph Pad Prism 8.0 software. The experimental data were expressed as mean  $\pm$  SD and the differences between multiple groups were marked by one way ANOVA.  $P < 0.05$  or  $P < 0.01$  indicated statistically significant difference.

## **Results**

### **Characterization of Doxil and CL-LIP**

Different sizes of Doxil were prepared by REV-extrusion and ammonium sulphate gradient method. As shown in **Fig 1 A&B**, sizes of Doxil were (101 $\pm$ 3.5) nm, (184 $\pm$ 3.9) nm, and (350 $\pm$ 20.4) nm, with the corresponding polydispersity index (PDI) values being 0.218 $\pm$ 0.005, 0.215 $\pm$ 0.004, 0.248 $\pm$ 0.008 and zeta potentials being (-12.28 $\pm$ 1.75) mV, (-12.83 $\pm$ 1.46) mV, (-13.01 $\pm$ 2.00) mV, respectively, all indicating negative zeta potential values. The encapsulation efficiency (EE%) and drug loading (DL%) of doxorubicin in different sizes of Doxil were listed in Supporting Information **Table S1**. Three sizes of Doxil all possessed high EE(%) of around 95-99% and DL(%) up to 7.5%, showing that liposomes prepared by the present method could efficiently encapsulate doxorubicin.



In order to investigate the stability of three sizes of Doxil, we stored them at 4°C for a week and measured the particle size and PDI values on the 1<sup>st</sup>, 3<sup>rd</sup>, 5<sup>th</sup> and 7<sup>th</sup> day by a Malvern dynamic light scatterer. As is shown in **Fig 1 C&D**, the particle size and PDI values of Doxil of about 101 and 108 nm remained almost invariant for at least 7 days, while the size and PDI of Doxil about 350 nm showed an increase at 7<sup>th</sup> day, suggesting good stability of Doxil with sizes under 200 nm. PDI values of liposomes with larger size, such as 350 nm or above, had a tendency to rise with prolonged storage time, indicating a poorer stability. Therefore, we chose to prepare Doxil with size of about 200 nm according to its stability and better macrophages intake *in vitro* and *in vivo* (**Supporting Information Fig S1 G&H**).

*In vitro* drug release of 3 sizes of Doxil was performed in PBS and determined by fluorescence values (**Fig 1 E**). Within 0.5h, *in vitro* cumulative release rates of ~100, ~180, ~350 nm Doxil at pH 7.4 were 28.04%, 17.52% and 37.96%, respectively, which met the requirements of the Chinese Pharmacopoeia that the cumulative release rates of liposomes in 0.5 h at the beginning should be lower than 40%. We could come to the conclusion that there was good release effect and no sudden release in the three kinds of Doxil *in vitro*.

To kill macrophages, CL-LIP was prepared using thin film hydration-extrusion method with a size of about 200 nm, a PDI around 0.056 and a zeta potential of  $-36.6 \pm 2.5$  mV (**Fig 1 F**). The concentration of clodronate in CL-LIP was 5.6 mg/mL as detected by ultraviolet spectroscopy. The EE% and DL% of CL-LIP around 200 nm were listed in **Supporting Information Table S2**. Both of EE% and DL% were low, but the clodronate liposomes prepared could still reach a certain level of concentration for administration.

Besides, the TEM images in **Fig 1 G&H** showed that both Doxil and CL-LIP (~150-200 nm) were spherical in morphology and shapes, revealing representative appearance of the liposomes. All the results suggested that doxorubicin and clodronate liposomes prepared by us had the characters of negative zeta potential values, narrow size distributions (sizes dispersed in water ranging from 100 to 350 nm) and good stability.

### **Combination of Doxil and CL-LIP Inhibits Hepatocarcinogenesis**

Prior to formal administration, appropriate size and dosage were determined by intra-spleen injection of different dosages of Doxil (1,2,4 mg/kg) and CL-LIP (1,5,15,35,45 mg/kg) to rats fed with DEN for 12 weeks. As is shown in **Supporting Information Fig S1**, the Doxil dosage of 2 mg/kg and 4 mg/kg effectively reduced tumor numbers and liver injuries, but 4 mg/kg groups showed distinct heart toxicity. In **Supporting Information Fig S2**, rats in the CL-LIP groups of 35, 45 mg/kg showed obvious elevations of serum ALT, AST and sudden decrease in ALB, suggesting intra-spleen injection of high concentration of CL-LIP would cause injuries and damage to liver function. In brief, we finally decided to inject Doxil at the dosage of 2 mg/kg and CL-LIP at 15 mg/kg in the following *in-vivo* administration for the sake of safety. Both liposomes were prepared in the size of ~200 nm for good stability and capacity of being captured by macrophages.

According to our previous study, rats exposed to 0.1% DEN in their drinking water for 12 weeks provided a primary HCC model before hepatocarcinogenesis(22). Doxil and CL-LIP were administered into the spleen once a week from 8<sup>th</sup> to 11<sup>th</sup> week to explore the effects of combination of liposomes in the stage of HCC initiation (**Fig 2 A**). Rats were divided into four groups: a. DEN; b. DEN+CL-LIP; c. DEN+Doxil; and d. DEN+CL-LIP+Doxil. The rats in DEN group received the same amount of saline as other liposomes groups by intra-spleen injection. As **Fig 2 B** displays, the liver surface of rats in DEN+Doxil group was rough with nodules, while the liver texture of rats in Doxil+CL-LIP group was not significantly abnormal and nearly no tumors were observed. Importantly, at the 12<sup>th</sup> week, there was obvious difference concerning the tumor incidence between DEN+Doxil+CL-LIP group and others (**Fig 2 C**). Also, rats in combination group showed the least number of tumors (**Fig 2 D**). For further HCC marker identification, we performed immunohistochemical staining of H&E and Alpha fetoprotein (AFP) in livers.

Besides, livers in four groups were collected for histopathological examination to further analyze hepatocarcinogenesis states. As **Fig 2 E** shows, in the DEN and CL-LIP group, tumor cells showed pleomorphism, enlarged nuclei, less cytoplasm and more abnormal nuclei. In addition, the tumor was well demarcated from the paracancer tissue, with obvious inflammatory cell infiltration and steatosis. Nevertheless, in the Doxil group, no tumor was observed visually, but the liver cells were in disorder and tumor nodules appeared. In Doxil+ CL-LIP group, liver cells were neatly arranged, nuclear size was in uniform, with no degeneration or necrosis, and the liver lobule structure was clear without inflammatory infiltration.

AFP was positively expressed in the cytoplasmic granular. **Fig 2 F** qualitatively showed that AFP expression was positive in the liver of control (DEN), CL-LIP and Doxil groups, while no evident AFP expression cells were seen in the liver of Doxil+CL-LIP group. The possible explanation was that the intervene by combining Doxil and CL-LIP could inhibit hepatocarcinogenesis induced by DEN in rats. However, injection of Doxil or CL-LIP alone was not able to achieve the same good effects when combining the two kinds of liposomes.

### **Doxil mixed with CL-LIP Inhibits HPCs Activation Before Hepatocarcinogenesis**

Hepatic progenitor cells (HPCs) are the original cells of hepatocarcinoma cells(23). At the initial stage of HCC, macrophages and HPCs interact to promote hepatocellular carcinoma(24). We had already seen the inhibition against hepatocarcinogenesis and depletion of macrophages by combination of Doxil and CL-LIP. To further observe whether the treatment affected HPCs' activation, the immunohistochemical staining of OV6 and cytokeratin 19(CK19), both well-known HPC markers(25), was performed. **Fig 3 A&B** implied that CL-LIP and Doxil+CL-LIP reduced OV6 positive cells, possibly by killing macrophages in the liver, and the mixed liposomes resulted in a more evident decrease. In **Fig 3 C&D**, it was apparent that there was less CK19+ cells in all the treatment groups, and combination of Doxil and CL-LIP group indicated the least expression of CK19+ cells, the reason behind may be that Doxil also restrained the activation and proliferation of HPCs and played a synergetic role with CL-LIP, which leading to the distinct inhibition of HPCs and HCC in different groups, especially Doxil+CL-LIP group.

## Doxil and CL-LIP's Combination Depletes Macrophages and Makes DOX Concentrated in Plasma Before Hepatocarcinogenesis

Our above results demonstrated that combination of Doxil and CL-LIP at an appropriate concentration could inhibit hepatocarcinogenesis. It was reported that macrophages and inflammation contributed to the liver neoplasia(26). To further investigate different treatment effects on overall macrophages in the liver, we performed the immunohistochemical staining to detect CD68, the typical marker of macrophages in the liver(27) and made quantitative statistics of immunohistochemistry images. Values of mean density (IOD/Area) in CL-LIP and Doxil+CL-LIP groups were less than those in the control and Doxil groups, but CL-LIP group showed no significant difference with Doxil group, while the mixed liposomes group implied that combination of Doxil+CL-LIP enhanced the macrophage-depletion effects of clodronate liposomes (**Fig 4 A&B**).

As demonstrated in **Fig 4 C**, CL-LIP had a negative influence on activities of NR8383 and rat peritoneal macrophages in a dose dependent manner. In accordance with the above results, the flow cytometry presented that CL-LIP was able to kill rat peritoneal macrophages, and the higher the concentration of CL-LIP, the more macrophages apoptosis (**Fig 4 D&E**). Conclusion could be drawn definitely that CL-LIP depletes macrophages not only *in vivo* but also *in vitro*.

Next, we intended to know more about the effects of CL-LIP on Doxil bio-distribution. We set three groups: a. Free drugs doxorubicin (Free Dox); b. Doxil; and c. Doxil+CL-LIP. Rats in these groups received different forms of doxorubicin including free drugs, liposomes and synergetic liposomes through the spleen. At specific time points, rats were sacrificed and HPLC-MS equipment was used to analyze the concentration of doxorubicin in their plasma and main organs to generate photos in **Fig 4 F-K** at last. Charts in **Fig 4 F-J** prompt liposomes, Doxil or Doxil+CL-LIP, avoided a wide distribution of doxorubicin in vital organs and tissues. Hence the nanocarrier liposomes effectively reduced toxicity and side effects in livers, spleens, lungs and kidneys, and in particular Doxil+CL-LIP caused no obvious damage to the heart and other vital organs (**Supporting Information Fig S3**). The results suggested Doxil+CL-LIP injected through the spleen also exerted plasma targeted concentration *in vivo* and could reach a double (from 2.5 to 6.1 mg/mL) plasma concentration than using Doxil alone. What's more, the plasma AUC of DOX in Doxil+CL-LIP group also exceeded that of the other two groups, with a value of 14 mg/L\*h compared with 4.9 mg/L\*h (Doxil) and 0.09 mg/L\*h (Free DOX). In another aspect, line charts of **Fig 4 F-K** manifest changes of doxorubicin concentration in the heart, liver, spleen, lung, kidney and plasma from 10 min to 48 h respectively, showing that free doxorubicin was quickly eliminated from the kidney within 4 hours and Doxil or Doxil+CL-LIP remained in the liver and spleen for longer time compared with other organs. Generally, CL-LIP affected the bio-distribution of Doxil and led to more remarkable retention effects of liposomes in the liver and spleen, mainly by increasing the MRT.

## Synergetic Administration of Doxil and CL-LIP Inhibits Progression of Hepatocarcinoma

Our previous reports showed that the period from 10<sup>th</sup> to 17<sup>th</sup> week was the progression and deterioration stage in DEN-induced HCC models(28). In order to investigate the therapeutic action of combination of the two kinds of liposomes, rats were subleased as mentioned above into DEN, DEN+CL-LIP, DEN+Doxil and DEN+CL-LIP+Doxil groups, and administered with different drugs by intra-spleen injection at the dosage of 2 mg/kg for Doxil and 15 mg/kg for CL-LIP once a week from 14<sup>th</sup> to 17<sup>th</sup> week during HCC development (**Fig 5 A**). We can see from **Fig 5 B to E** that though in 19<sup>th</sup> week the occurrence of tumors was inevitable, there was evident diversity among control and another three groups in liver morphology, tumor numbers and maximum tumor sizes. Interestingly, Doxil+CL-LIP still demonstrated significant therapeutic effects on rats in HCC progression stage.

As for **Fig 5 F**, evidently, there was no complete hepatic lobule structure and liver cells were in disorder in the DEN and DEN+CL-LIP groups, with pleomorphic cells, enlarged nuclei, less cytoplasm, and more deformed nuclei. The treatments with Doxil and combination of Doxil+CL-LIP improved the pathological abnormal structure of livers. In brief, the combination of Doxil and CL-LIP significantly killed macrophages and reduced liver injuries caused by DEN, inhibiting HCC at the tumor progression stage.

The survival curves (Kaplan-Meier plot) of DEN-induced (14 weeks) rats treated with saline (DEN group), CL-LIP, Doxil and Doxil+CL-LIP were shown in **Fig 5 G**. No remarkable influence was observed on rat survival time in combination of Doxil+CL-LIP groups and other groups of during this period.

### **Mixed Doxil and CL-LIP Depletes Macrophages During Progression of Hepatocarcinoma**

Aiming to analyze the antineoplastic mechanism of combining liposomes in the progression stage, we then subjected the liver sections to immunohistochemical staining of CD68, detecting the expression level of CD68+ macrophages. The staining images and statistics of IOD/Area had shown that CL-LIP and Doxil+CL-LIP groups had macrophages depletion effects in the liver, and the latter group showed better elimination effect for macrophages (**Fig 6 A&B**).

### **Doxil Combined with Clodronate Liposome Induces Tumor Cell Apoptosis**

Our results above verified that combination of Doxil and CL-LIP could efficiently deplete macrophages and attenuated HCC initiation and progression. Macrophages are known to capture objects with larger size such as liposomes of clodronate and doxorubicin(29). After the death of macrophages, whether the chemotherapeutic drug, doxorubicin, was released and affected the surrounding tumor cells? Here we chose CCK-8 assay to examine the influences of mixed liposomes on the viability of rat liver cancer cells RH35 and performed Tunnel staining on rat livers in DEN, DEN+CL-LIP,

DEN+Doxil and DEN+Doxil+CL-LIP groups at 19 weeks. *In vitro*, cell viability in Doxil+CL-LIP group decreased apparently (**Fig 7 A**) and simultaneously, Tunel-positive cells demonstrated a significant rise in percentage in Doxil+CL-LIP group (**Fig 7 B**), indicating that combination of Doxil and CL-LIP induced tumor cell apoptosis, protecting livers from HCC progression.

## Discussion

Mononuclear phagocytic system (MPS) has strong phagocytosis and defense function *in vivo*. Liver and spleen are the main organs of MPS. Macrophages, the main cell composition of MPS, are critical in clearance of pathogen, maintenance of homeostasis, immune surveillance, and responses to infection and inflammation(4, 30). The liver contains the majority of resident macrophages, Kupffer cells, and makes up over 80% of systemic MPS(31, 32). Kupffer cells play a major role in clearance of foreign matter *in vivo*, and nanoparticles injected intravenously are often captured in the liver(33–35). Moreover, macrophages and inflammatory microenvironment are also keys in initiation and deterioration of liver cancer(7–10). Activated Kupffer cells release cytokines and/or reactive oxygen species, inducing hepatocyte proliferation and enhancing clonal expansion of pretumor cells, finally causing neoplasia(10).

Aiming to target macrophages and deliver chemotherapy drug to the liver, we prepared liposomes containing doxorubicin, and a specific macrophage depletion drug, clodronate. Free clodronate shows no toxicity and very short half-life in circulation, but once it is transported into the cells by liposomes and accumulates to certain concentration, toxic ATP analogues will be formed, resulting in intracellular energy metabolism disorders and apoptosis(36–38). Following the preparation, we investigated the therapeutic effects of combination of doxorubicin and clodronate liposomes (Doxil + CL-LIP) on HCC of early and advanced phase. Our results showed that clodronate liposomes successfully induced the death of macrophages in the liver, and combination with doxorubicin liposomes at a low dose of 2 mg/kg effectively inhibited the initiation and progression of liver cancer, without evident injuries to other main organs like the heart, spleen or kidney, greatly reducing the systemic side effects and heart toxicity of free doxorubicin(39).

Due to the influence of MPS, characteristics of liposomes, especially the particle sizes, determine their final biological distribution after entering the body. For liposomes with a diameter of 50–100 nm, they can penetrate and accumulate in tumor tissues depending on the enhanced permeability and retention effect (EPR). Larger particles (> 150 nm), especially those attached to conditioning proteins, will be recognized and captured by MPS(29, 32, 40, 41). An analysis of 117 papers about nanomedicine published in the last decade showed that 99% of injected circulating nanoparticles were isolated and removed by MPS, and only 0.7% were ultimately delivered to the tumor site(42). In this study, we prepared doxorubicin and clodronate liposomes and chose the larger and stable size of about 200 nm to make it easier to be captured by MPS, and to accumulate and deplete macrophages sufficiently. Liposomes of 200 nm were locally injected into the spleen and were expected to be captured by MPS in the liver and spleen(28, 43). The results of bio-distribution showed that 10–30 minutes after intra-spleen administration of Doxil and CL-LIP, other than plasma, the concentration of DOX in the liver was the highest among all the main organs. DOX could maintain certain concentration in the liver and spleen for the longest time (up to 20–21 hours), which was in accord with our expectations. In this study we prepared liposomes of larger size and injected them through the spleen on purpose, expecting liposomes to be passively phagocytized by macrophages in MPS of the spleen and liver, and finally to kill macrophages when delivered simultaneously with chemotherapy drugs. It may be an easier and valid

method for administration of traditional chemotherapy drugs like doxorubicin, to improve the therapeutic efficacy without evident toxic or side effects.

During the hepatocarcinogenesis and HCC progression stages, combination of doxorubicin and clodronate liposomes notably decreased liver macrophages. It is believed that targeting and depleting macrophages in the liver may effectively inhibit the hepatocarcinogenesis and improve therapeutic effect of drugs delivered by nanocarriers<sup>46</sup>. When HCC aggravates, CL-LIP-induced depletion of macrophages in the liver, including tumor associated ones, would improve the suppression of TME and make Doxil that were captured by macrophages released again to kill tumor cells, finally leading to apoptosis of more tumor cells in terminal cancer compared with DEN + Doxil group. On the other hand, we could see that Doxil also played a certain role in macrophage clearance, probably due to apoptosis of macrophages after phagocytosis of doxorubicin. We speculate that the clearance of macrophages could lead to greater chance for Doxil to be internalized by proliferating tumor cells, and could maintain doxorubicin at a sustainable higher level in the plasma.

However, there are also some limitations in our research. Further study needs to be done to examine the activation and proliferation of hepatic progenitor cells (HPCs) in HCC initiation stage. We found that HPCs activation could be inhibited by clodronate liposomes before hepatocarcinogenesis. The possible explanation is the death of total macrophages in the liver, including Kupffer cells and blood monocyte-derived macrophages (MDM)(24), which could attenuate liver injuries and reduce the proliferation of HPCs. HPCs as the tumor-initiating cells involved in liver cancer are influenced by macrophages/Kupffer cells(23, 24, 44). More details and association between macrophages depletion and HPCs down-regulation also need to be explored. Meanwhile, observation of recovery time of macrophages after depletion are lacking.

## Conclusions

In conclusion, the combination of doxorubicin and clodronate liposomes accumulated in the liver and spleen and effectively reduced macrophages, making DOX stay at a higher concentration in the plasma and inhibiting activation of HPCs, finally exerting preventive and therapeutic actions on rat HCC models, without evident side effects. Application of two kinds of simple and convenient liposomes in a topical administration way has demonstrated surprising inhibition against HCC by targeting macrophages in the liver, further regulating and improving TME, which may provide a new and economical strategy for chemotherapy of HCC.

## Abbreviations

HCC: Hepatocellular carcinoma; DEN: Diethylnitrosamine; Doxil: Doxorubicin-liposome; CL-LIP: Clodronate-liposome; DOX: Doxorubicin; HPCs: Hepatic progenitor cells; MPS: Mononuclear phagocytic system; TAM: Tumor-associated macrophage; DNA: Deoxyribonucleic acid; CD68: Cluster of Differentiation 68; CD163: Cluster of Differentiation 163; iNOS: inducible Nitric Oxide Synthase; AFP:

Alpha-fetoprotein; OV6: Oval cell marker 6; FITC: Fluorescein isothiocyanate; CCK8: Cell counting Kit-8; ELISA: Enzyme Linked Immunosorbent Assay; SD: Sprague-Dawley; REV: Reverse phase Evaporation Vesicle; HPLC: High Performance Liquid Chromatography; EE: Encapsulation Efficiency; DL: Drug Loading; PDI: Particle Dispersion Index; PBS: Phosphate Buffer Saline; FBS: Foetal Bovine Serum; CO<sub>2</sub>: Carbon dioxide; LSCM: Laser Scanning Confocal Microscopy; IF: Immunofluorescence; H&E: Hematoxylin and Eosin; ALT: Alanine transaminase; AST: Aspartate transaminase; ALB: Albumin; IVC: Individual Ventilated Cages; TUNEL: Terminal Deoxynucleotidyl Transferase-mediated dUTP-biotin Nick End Labeling; HPLC-MS: High Performance Liquid Chromatography-Mass Spectrometry; IOD: Integral Optical Density; EPR: Enhanced permeability and retention effect; MDM: Monocyte-derived macrophages.

## **Declarations**

### **Ethics approval and consent to participate**

Ethical approval was obtained from the Naval Medical University Ethics Committee. All animal protocols used were approved by the Institutional Animal Care and Use Committee of the Institute of Health Sciences.

### **Consent for publication**

Not applicable.

### **Availability of data and materials**

The datasets used and/or analyzed during the current study are available from the corresponding author on reasonable request.

### **Competing interests**

The authors declare no conflicts of interest.

### **Funding**

This study was supported by the National Key R&D Program of China (Grant NO. 2018YFA0107500, 2017YFA0504503); National Natural Science Foundation of China (Grant NO. 81872243, 81972599, 82073032, 82073037, 82173276); The municipal medical-enterprise collaborative clinical trial management project of Shanghai Shenkang Hospital Development Center (20CR4008B); The guaranteed discipline promotion project of Changhai Hospital (2020YBZ011); and Shanghai Municipal Health Bureau (Grant NO. 20214Y0013).

### **Author contributions**

Li Zhang and Lixin Wei conceived and designed the work. Dandan Sheng, Gangqi Sun, Luyao Zhang, Hengyan Zhang and Xinxia Wang performed the experiments. Hengyan Zhang wrote the paper and

Xiaojuan Hou, Xue Yang arranged the graphics. Li Zhang, Lixin Wei, Zhipeng Han, Xue Yang, Xiaojuan Hou and Ying Lu commented and corrected the paper. All of the authors have read and approved the final manuscript.

## Acknowledgements

Not applicable.

## Authors' information

<sup>1</sup> Clinical Research Unit, Changhai Hospital, Naval Medical University, 168 Changhai Road, Shanghai 200433, China. <sup>2</sup> Pharmaceutical Department, PLA Strategic Support Force Medical Center, No.9Anxiangbeili Road, Chaoyang District, Beijing 100101, China. <sup>3</sup> Tumor Immunology and Gene Therapy Center, Third Affiliated Hospital of Second Military Medical University, 225 Changhai Road, Shanghai 200438, China. <sup>4</sup> The National Center for Liver Cancer, Shanghai 201805, China. <sup>5</sup> Shanghai International Medical Center, Shanghai International Medical Center, 4358 Kangxin Road, Shanghai 201315, China. <sup>6</sup> Department of Pharmaceutical Sciences, School of pharmacy, Naval Medical University, 325 Guohe Road, Shanghai 200433, China.

## References

1. Al-Jamal WT, Kostarelos K. Liposomes: from a clinically established drug delivery system to a nanoparticle platform for theranostic nanomedicine. *Acc Chem Res.* 2011;44(10):1094-104.
2. Antimisiaris SG, Marazioti A, Kannavou M, Natsaridis E, Gkartziou F, Kogkos G, et al. Overcoming barriers by local drug delivery with liposomes. *Advanced drug delivery reviews.* 2021;174(Jul):53-86.
3. Gregory SH, Wing EJ. Neutrophil-Kupffer-cell interaction in host defenses to systemic infections. *Immunol Today.* 1998;19(11):507-10.
4. Davies LC, Jenkins SJ, Allen JE, Taylor PR. Tissue-resident macrophages. *Nat Immunol.* 2013;14(10):986-95.
5. Liaskou E, Wilson DV, Oo YH. Innate immune cells in liver inflammation. *Mediators Inflamm.* 2012;2012:949157.
6. Zhou S, Gu J, Liu R, Wei S, Wang Q, Shen H, et al. Spermine Alleviates Acute Liver Injury by Inhibiting Liver-Resident Macrophage Pro-Inflammatory Response Through ATG5-Dependent Autophagy. *Front Immunol.* 2018;9:948.
7. Jiang J, Wang GZ, Wang Y, Huang HZ, Li WT, Qu XD. Hypoxia-induced HMGB1 expression of HCC promotes tumor invasiveness and metastasis via regulating macrophage-derived IL-6. *Exp Cell Res.* 2018;367(1):81-8.
8. Li XF, Chen C, Xiang DM, Qu L, Sun W, Lu XY, et al. Chronic inflammation-elicited liver progenitor cell conversion to liver cancer stem cell with clinical significance. *Hepatology.* 2017;66(6):1934-51.



9. Manifold IH, Triger DR, Underwood JC. Kupffer-cell depletion in chronic liver disease: implications for hepatic carcinogenesis. *Lancet*. 1983;2(8347):431-3.
10. Roberts RA, Ganey PE, Ju C, Kamendulis LM, Rusyn I, Klaunig JE. Role of the Kupffer cell in mediating hepatic toxicity and carcinogenesis. *Toxicol Sci*. 2007;96(1):2-15.
11. Barnett FH, Rosenfeld M, Wood M, Kiosses WB, Usui Y, Marchetti V, et al. Macrophages form functional vascular mimicry channels in vivo. *Sci Rep*. 2016;6:36659.
12. Li X, Yao W, Yuan Y, Chen P, Li B, Li J, et al. Targeting of tumour-infiltrating macrophages via CCL2/CCR2 signalling as a therapeutic strategy against hepatocellular carcinoma. *Gut*. 2017;66(1):157-67.
13. Wu K, Kryczek I, Chen L, Zou W, Welling TH. Kupffer cell suppression of CD8+ T cells in human hepatocellular carcinoma is mediated by B7-H1/programmed death-1 interactions. *Cancer Res*. 2009;69(20):8067-75.
14. Qiu L, Qiao M, Chen Q, Tian C, Long M, Wang M, et al. Enhanced effect of pH-sensitive mixed copolymer micelles for overcoming multidrug resistance of doxorubicin. *Biomaterials*. 2014;35(37):9877-87.
15. Li Z, Wang F, Li Y, Wang X, Lu Q, Wang D, et al. Combined anti-hepatocellular carcinoma therapy inhibit drug-resistance and metastasis via targeting "substance P-hepatic stellate cells-hepatocellular carcinoma" axis. *Biomaterials*. 2021;276:121003.
16. Van Rooijen N, Sanders A. Kupffer cell depletion by liposome-delivered drugs: comparative activity of intracellular clodronate, propamidine, and ethylenediaminetetraacetic acid. *Hepatology*. 1996;23(5):1239-43.
17. Shah SM, Goel PN, Jain AS, Pathak PO, Padhye SG, Govindarajan S, et al. Liposomes for targeting hepatocellular carcinoma: use of conjugated arabinogalactan as targeting ligand. *Int J Pharm*. 2014;477(1-2):128-39.
18. Szoka F, Jr., Papahadjopoulos D. Procedure for preparation of liposomes with large internal aqueous space and high capture by reverse-phase evaporation. *Proc Natl Acad Sci U S A*. 1978;75(9):4194-8.
19. Zucker D, Marcus D, Barenholz Y, Goldblum A. Liposome drugs' loading efficiency: a working model based on loading conditions and drug's physicochemical properties. *J Control Release*. 2009;139(1):73-80.
20. Van Rooijen N, Sanders A. Liposome mediated depletion of macrophages: mechanism of action, preparation of liposomes and applications. *J Immunol Methods*. 1994;174(1-2):83-93.
21. van Rooijen N, van Kesteren-Hendriks E. "In vivo" depletion of macrophages by liposome-mediated "suicide". *Methods Enzymol*. 2003;373:3-16.
22. Zong C, Zhang H, Yang X, Gao L, Hou J, Ye F, et al. The distinct roles of mesenchymal stem cells in the initial and progressive stage of hepatocarcinoma. *Cell Death Dis*. 2018;9(3):345.
23. Sia D, Villanueva A, Friedman SL, Llovet JM. Liver Cancer Cell of Origin, Molecular Class, and Effects on Patient Prognosis. *Gastroenterology*. 2017;152(4):745-61.

24. Elsegood CL, Chan CW, Degli-Esposti MA, Wikstrom ME, Domenichini A, Lazarus K, et al. Kupffer cell-monocyte communication is essential for initiating murine liver progenitor cell-mediated liver regeneration. *Hepatology*. 2015;62(4):1272-84.
25. Castro-Gil MP, Sanchez-Rodriguez R, Torres-Mena JE, Lopez-Torres CD, Quintanar-Jurado V, Gabino-Lopez NB, et al. Enrichment of progenitor cells by 2-acetylaminofluorene accelerates liver carcinogenesis induced by diethylnitrosamine in vivo. *Mol Carcinog*. 2021;60(6):377-90.
26. Wan S, Kuo N, Kryczek I, Zou W, Welling TH. Myeloid cells in hepatocellular carcinoma. *Hepatology*. 2015;62(4):1304-12.
27. Taylor PR, Martinez-Pomares L, Stacey M, Lin HH, Brown GD, Gordon S. Macrophage receptors and immune recognition. *Annu Rev Immunol*. 2005;23:901-44.
28. Kai MP, Brighton HE, Fromen CA, Shen TW, Luft JC, Luft YE, et al. Tumor Presence Induces Global Immune Changes and Enhances Nanoparticle Clearance. *ACS Nano*. 2016;10(1):861-70.
29. Ishida T, Harashima H, Kiwada H. Liposome clearance. *Biosci Rep*. 2002;22(2):197-224.
30. Motwani MP, Gilroy DW. Macrophage development and polarization in chronic inflammation. *Semin Immunol*. 2015;27(4):257-66.
31. Biozzi G, Benacerraf B, Halpern BN, Stiffel C, Hillemand B. Exploration of the phagocytic function of the reticuloendothelial system with heat denatured human serum albumin labeled with I131 and application to the measurement of liver blood flow, in normal man and in some pathologic conditions. *J Lab Clin Med*. 1958;51(2):230-9.
32. Harashima H, Sakata K, Funato K, Kiwada H. Enhanced hepatic uptake of liposomes through complement activation depending on the size of liposomes. *Pharm Res*. 1994;11(3):402-6.
33. Desai N. Challenges in development of nanoparticle-based therapeutics. *AAPS J*. 2012;14(2):282-95.
34. Sadauskas E, Wallin H, Stoltenberg M, Vogel U, Doering P, Larsen A, et al. Kupffer cells are central in the removal of nanoparticles from the organism. *Part Fibre Toxicol*. 2007;4:10.
35. Gaumet M, Vargas A, Gurny R, Delie F. Nanoparticles for drug delivery: the need for precision in reporting particle size parameters. *Eur J Pharm Biopharm*. 2008;69(1):1-9.
36. Moreno SG. Depleting Macrophages In Vivo with Clodronate-Liposomes. *Methods Mol Biol*. 2018;1784:259-62.
37. van Rooijen N. Extracellular and intracellular action of clodronate in osteolytic bone diseases? A hypothesis. *Calcif Tissue Int*. 1993;52(6):407-10.
38. van Rooijen N, van Kesteren-Hendriks E. Clodronate liposomes: perspectives in research and therapeutics. *J Liposome Res*. 2002;12(1-2):81-94.
39. Deepa K, Singha S, Panda T. Doxorubicin nanoconjugates. *J Nanosci Nanotechnol*. 2014;14(1):892-904.
40. Harashima H, Huong TM, Ishida T, Manabe Y, Matsuo H, Kiwada H. Synergistic effect between size and cholesterol content in the enhanced hepatic uptake clearance of liposomes through complement activation in rats. *Pharm Res*. 1996;13(11):1704-9.

41. Willekens FL, Werre JM, Kruijt JK, Roerdinkholder-Stoelwinder B, Groenen-Dopp YA, van den Bos AG, et al. Liver Kupffer cells rapidly remove red blood cell-derived vesicles from the circulation by scavenger receptors. *Blood*. 2005;105(5):2141-5.
42. Wilhelm S, Tavares AJ, Qin D, Ohta S, Chan W. Analysis of nanoparticle delivery to tumours. *Nature Reviews Materials*. 2016;1(5):16014.
43. Misawa R, Soeda J, Ise H, Takahashi M, Kubota K, Mita A, et al. Potential feasibility of early bone marrow cell injection into the spleen for creating functional hepatocytes. *Transplantation*. 2009;87(8):1147-54.
44. Viebahn CS, Benseler V, Holz LE, Elsegood CL, Vo M, Bertolino P, et al. Invading macrophages play a major role in the liver progenitor cell response to chronic liver injury. *Journal of Hepatology*. 2010;53(3):500-7.

## Figures

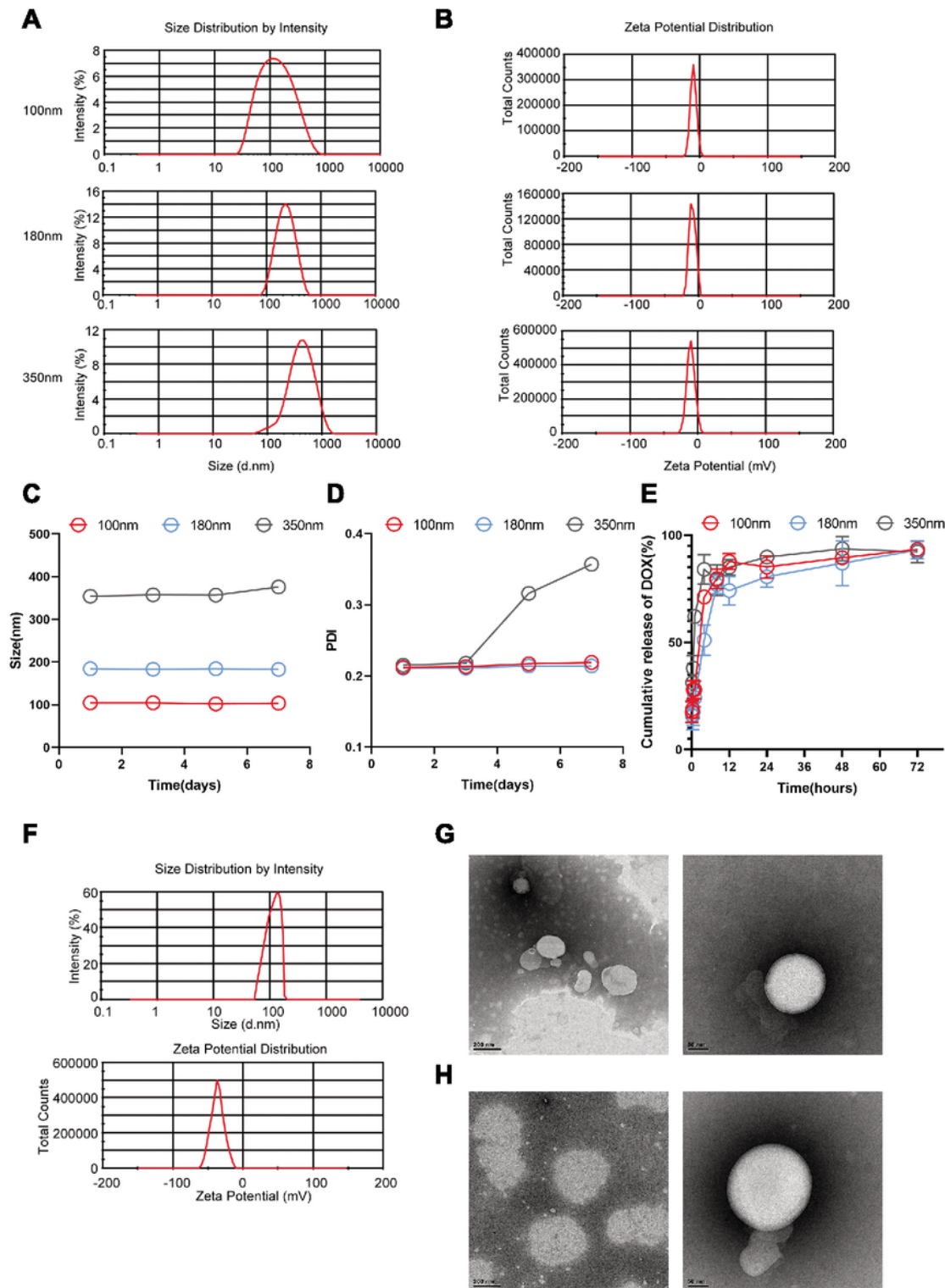


**Figure 1**

Characterization of Doxil and CL-LIP. (A)-(B) are hydrodynamic sizes and the zeta potentials of Doxil (100,180,350 nm); (C)-(D) indicate the stability of sizes and PDI of Doxil in a week; (E) shows the cumulative release of DOX from Doxil in vitro in 72 h. Data are mean  $\pm$  standard deviation (SD),  $n=3$ . (F) is hydrodynamic size and zeta potential of CL-LIP. (G)-(H) are TEM images of Doxil and CL-LIP. Scale bar = 100 nm (left)/ 50nm (right)

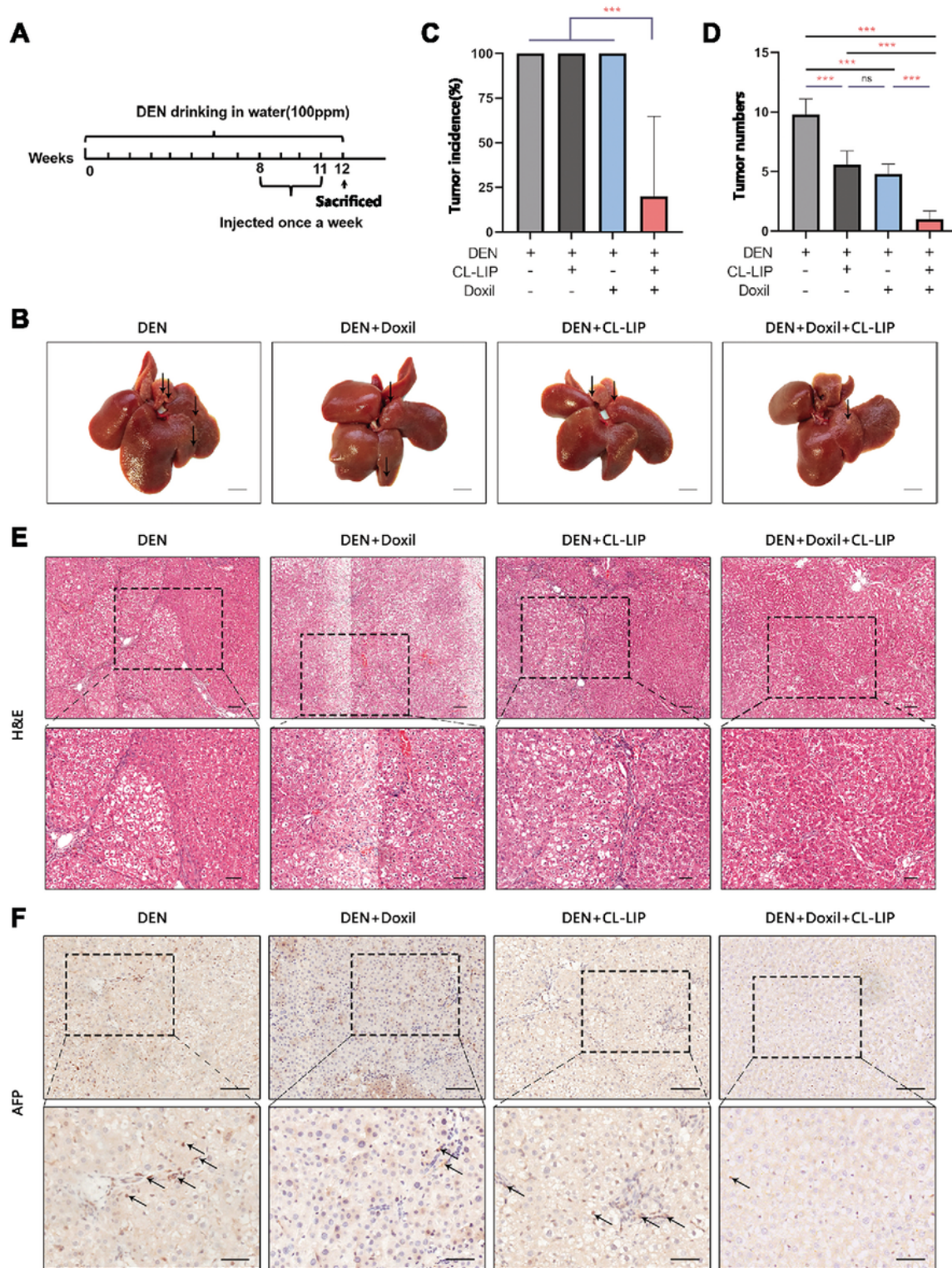


**Figure 2**

Combination of Doxil and CL-LIP inhibits hepatocarcinogenesis. (A) is a diagram of experimental protocol; rats were given DEN (0.1%, 95 mg/L) in drinking water for 12 weeks and were exposed to normal saline, Doxil, CL-LIP and Doxil + CL-LIP respectively by in tra-spleen injection once a week from 8th to 11th week. Livers were taken at 12 weeks. (B) shows gross appearance of livers in DEN, DEN+Doxil, DEN+CL-LIP and DEN+Doxil + CL-LIP groups at 12 weeks. Scale bar =1 cm. (C)-(D) indicate the tumor

incidence and tumor numbers of livers of rats after treatment with saline, Doxil, CL-LIP and Doxil + CL-LIP and sacrificed at 12 weeks. Data are mean  $\pm$  SD,  $n=5$ ; \*  $P<0.05$ , \*\*  $P<0.01$  and \*\*\*  $P<0.001$  vs. DEN/Doxil + CL-LIP. (E) is representative H&E staining appearance of livers from rats in DEN, Doxil, CL-LIP and Doxil + CL-LIP groups at 12 weeks. (F) are representative immunostaining images of Alpha-fetoprotein (AFP); the brown spots are AFP positive cells. Scale bar = 100  $\mu\text{m}$  (above) / 50  $\mu\text{m}$  (below).

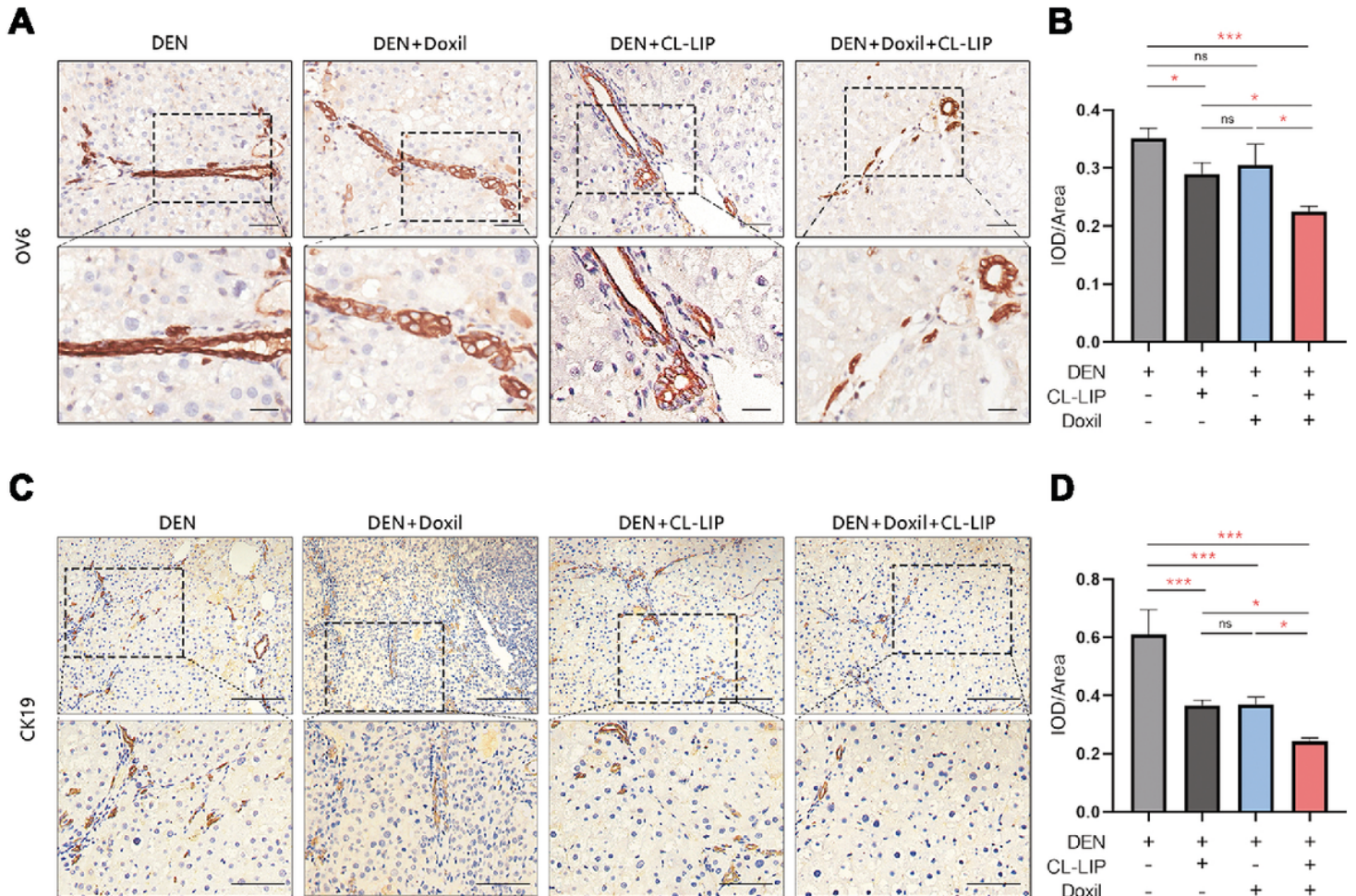


**Figure 3**

Combination of Doxil and CL-LIP inhibits HPCs activation before hepatocarcinogenesis. (A) are representative immunostaining images of OV6; the brown spots are OV6 positive cells. Scale bar = 50  $\mu\text{m}$  (above) / 25  $\mu\text{m}$  (below). (B) is quantitative IOD/Area analysis of OV6. (C) are representative immunostaining images of CK19; the brown spots are CK19 positive cells. Scale bar = 200  $\mu\text{m}$  (above) / 100  $\mu\text{m}$  (below). (D) shows quantitative IOD/Area analysis of CK19. Data are mean  $\pm$  SD,  $n=3$ ; \*  $P<0.05$ , \*\*\*  $P<0.001$  vs. DEN/Doxil + CL-LIP. ns, not significant.

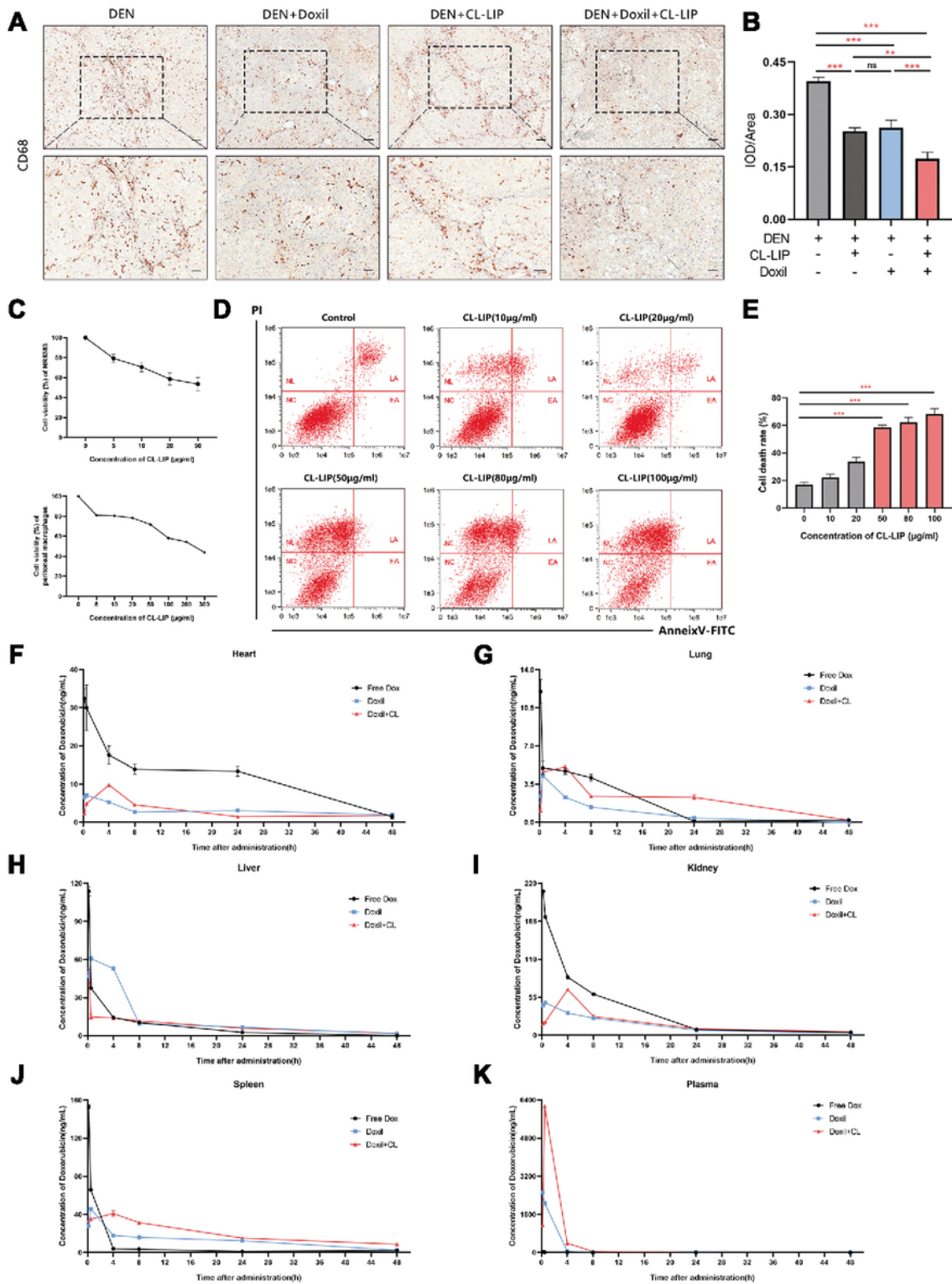


**Figure 4**

Combination of Doxil and CL-LIP depletes macrophages and makes DOX concentrated in plasma before hepatocarcinogenesis. (A) are representative immunostaining images of CD68 in livers from rats in DEN, Doxil, CL-LIP and Doxil + CL-LIP groups at 12 weeks; the brown spots are CD68 positive cells. Scale bar = 100  $\mu$ m (above) / 50  $\mu$ m (below). (B) is quantitative analysis of IOD/Area of CD68. Data are mean  $\pm$  SD,  $n=3$ ; \*\*  $P<0.01$ , \*\*\*  $P<0.001$  vs. DEN/Doxil + CL-LIP. ns, not significant. (C) shows cell viability of NR8383

(above) and rat peritoneal macrophages (below) measured by CCK8 assay; cells were treated with different concentrations of CL-LIP (5, 10, 20, 50, 100, 200 or 300 µg /mL) for 24 h. (D) indicates the apoptosis of rat peritoneal macrophages cells induced by CL-LIP at different concentrations were detected using FITC Annexin V-PI Apoptosis detection kit and measured by flow cytometry; (E) is the histogram representing the percentage of cell apoptosis. Data are mean ± SD,  $n=3$ , \*\*\*  $P<0.001$  vs. Control (0 mg/mL). (F)-(K) show *in vivo* bio-distribution of free doxorubicin, Doxil and Doxil + CL-LIP from 10 mins to 48 h after administration in DEN induced HCC rats at 8 weeks; concentration of doxorubicin and changes in heart, lung, liver, kidney, spleen and plasma were detected by HPLC-MS analysis. Doxil /Doxil combined with CL-LIP reduced distribution of doxorubicin in main organs and tissues; Doxil combined with CL-LIP exerted plasma-concentrated effects and maintained DOX concentration for longer time in liver and spleen.



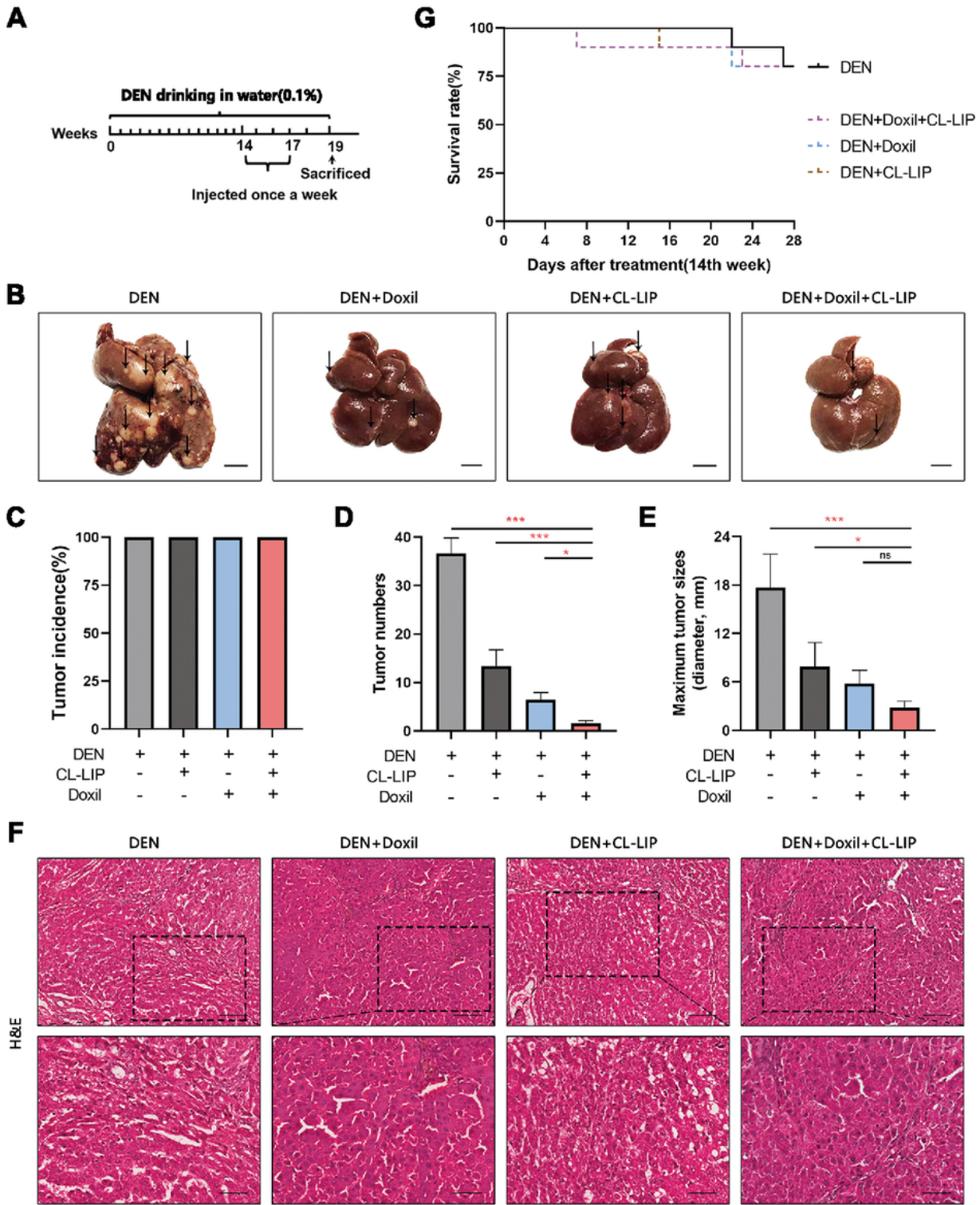


**Figure 5**

Combination of Doxil and CL-LIP inhibits progression of hepatocarcinoma. (A) is a diagram of experimental protocol; rats were given DEN (0.1%, 95 mg/L) in drinking water for 19 weeks and were exposed to normal saline, Doxil, CL-LIP and Doxil + CL-LIP respectively by intra-spleen injection once a week from 14th to 17th week. Livers were taken at 19 weeks. (B) shows gross appearance of livers in DEN, CL-LIP, Doxil and Doxil + CL-LIP groups at 19 weeks. Scale bar = 1 cm. (C)-(E) indicate the tumor

incidence, tumor numbers and maximum tumor sizes of livers of rats after treatment with saline, Doxil, CL-LIP and Doxil + CL-LIP and sacrificed at 19 weeks. Data are mean  $\pm$  SD,  $n=5$ ; \*  $P<0.05$ , \*\*\*  $P<0.001$  vs. DEN/Doxil + CL-LIP. ns, not significant. (F) is representative H&E staining appearance of livers from rats in DEN, Doxil, CL-LIP and Doxil + CL-LIP groups at 19 weeks. Scale bar = 100  $\mu\text{m}$  (above) / 50  $\mu\text{m}$  (below). (G) shows survival curves of DEN, DEN+Doxil/+CL-LIP/+Doxil+CL-LIP groups from administration of drugs,  $n=10$ .

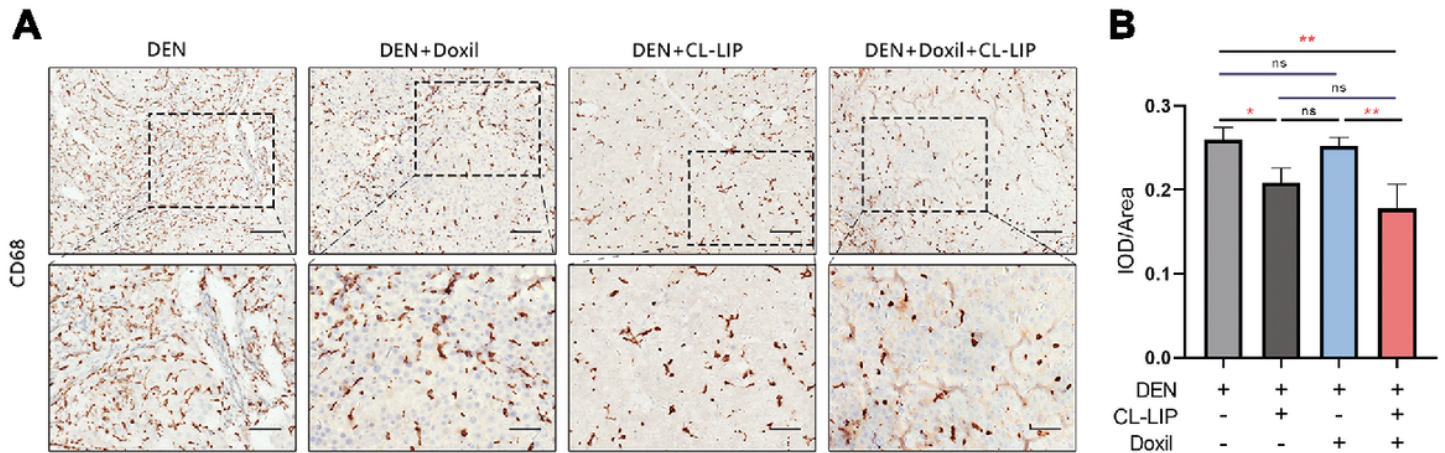


**Figure 6**

Combination of Doxil and CL-LIP depletes macrophages during progression of hepatocarcinoma. (A) are representative immunostaining images of CD68; the brown spots are CD68 positive cells. Scale bar = 100  $\mu\text{m}$  (above) / 50  $\mu\text{m}$  (below). (B) is quantitative analysis of IOD/Area of CD68 in livers from rats in DEN, Doxil, CL-LIP and Doxil + CL-LIP groups at 19 weeks. Data are mean  $\pm$  SD,  $n=3$ ; \*  $P<0.05$ , \*\*  $P<0.01$  vs. DEN/Doxil + CL-LIP. ns, not significant.

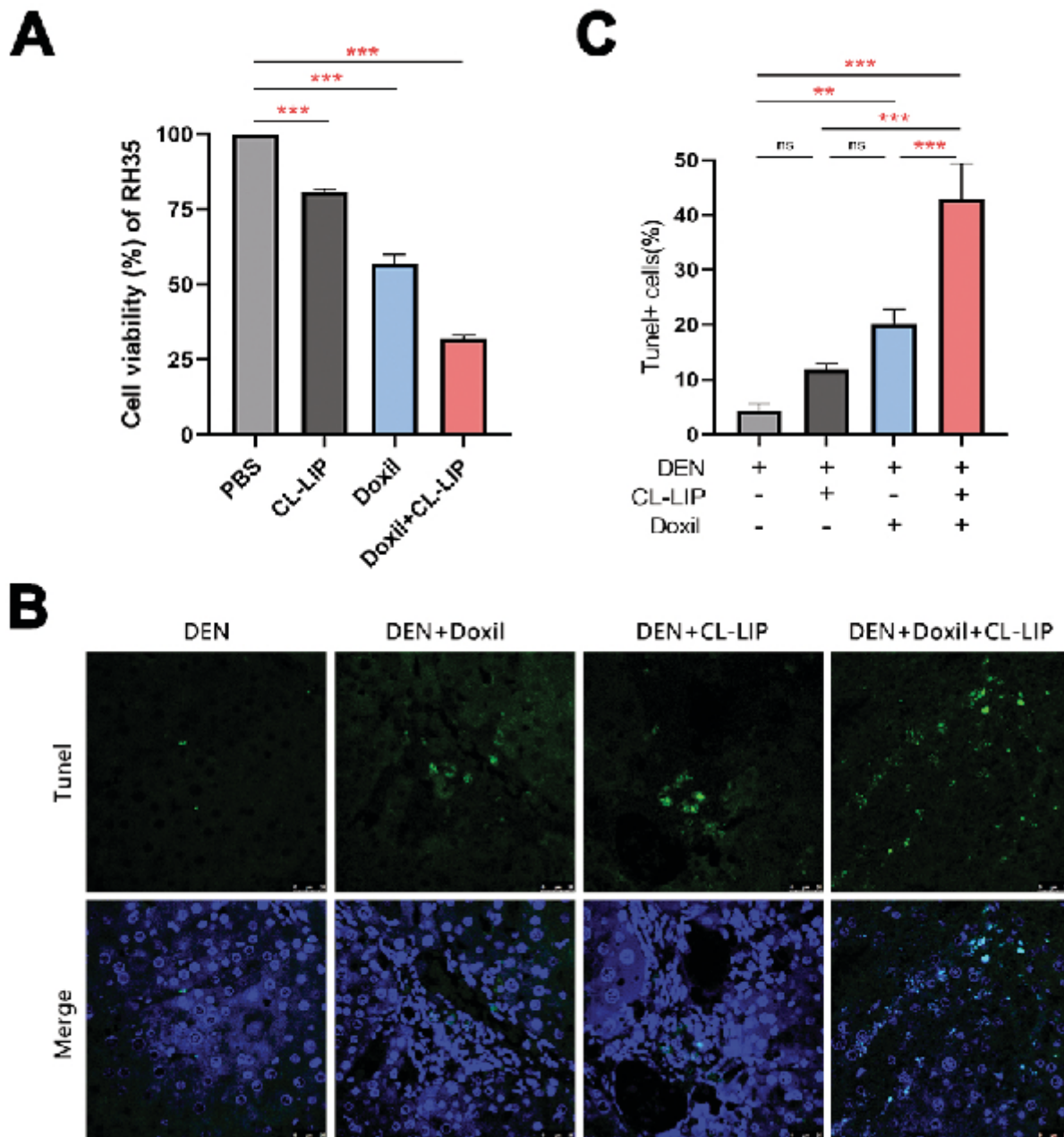


**Figure 7**

Combination of Doxil and CL-LIP induces tumor cell apoptosis. (A) shows cell viability of RH35 cells measured by CCK8 assay; RH35 cells were treated with PBS, CL-LIP (10 $\mu$ g/mL), Doxil(1 $\mu$ g/mL) and Doxil + CL-LIP for 24h respectively. (B) are Tunel staining images of rat livers in DEN, DEN+CL-LIP, DEN+Doxil and DEN+Doxil+CL-LIP groups at 19 weeks. Scale bar = 25  $\mu$ m. (C) is the semiquantitative analysis of Tunel staining images. Data are mean  $\pm$  SD,  $n=3$ ; \*\*  $P<0.01$ , \*\*\*  $P<0.001$  vs. Doxil + CL-LIP /DEN. ns, not significant.

## Supplementary Files

This is a list of supplementary files associated with this preprint. Click to download.

- [supplementarymaterials.docx](#)
- [Graphicabstract.docx](#)
- [FigS1.pdf](#)
- [FigS2.pdf](#)
- [FigS3.pdf](#)
- [Additionalfiles.docx](#)